

Wave Development on a Thinning Liquid Film

M. J. Holgate†

SUMMARY

Experimental results are presented for the growth of surface waves on a liquid film that thins as it flows under gravity over the surface of an upright circular cone. The characteristics of the mean film are calculated on the assumption of quasi-parallel flow, and the actual mean thickness found to relate very closely to that found on this basis. The development of the film was found to fall into three phases: the entry zone in which the velocity profile of the film becomes established where no waves are visible, a region of wave growth in which amplitude, wave speed, and wave length all grow, and a final region in which amplitude and wave speed decline as the film thins further although wave length continues to grow. An empirical relationship is presented which expresses the wave number at any point on the cone in terms of the flow rate and a parameter based on the local Reynolds and Weber numbers and cone angle. It was found that for a given flow rate the maximum wave amplitude was reached at a value of wave number of 0.048.

NOTATION

A_{rms}	root mean square amplitude
\hat{A}	peak amplitude
D	diameter of cone at point of measurement
(Fr)	Froude number = $\bar{u}/\sqrt{g\delta}$
g	gravitational acceleration
l	wave intensity = A_{rms}/δ
Q	volumetric flowrate
(Re)	Reynolds number = $\bar{u}\delta/\nu$
u	velocity at a general point in the film
\bar{u}	mean film velocity
(We)	Weber number = $\bar{u}\sqrt{\delta\rho/\sigma}$
x	distance along cone surface from apex
y	distance normal to cone surface
α	wave number = $2\pi\delta/\lambda$
β	semi-vertex angle of the cone
δ	mean film thickness
λ	wavelength
ν	kinematic viscosity
ρ	fluid density
σ	surface tension
ψ	= $(3/\cos\beta)^{1/6} (Re) (We)$
ψ'	= $[(\frac{2}{3}(Re) - \tan\beta)^3 (We)^2]/(Re)$

INTRODUCTION

The study, both theoretical and experimental, of the gravity-driven flow of thin liquid films has been confined to date almost exclusively to the flow over plane surfaces, or over vertical cylinders whose diameters are large compared with the film thickness. In such cases, there is an initial entry zone during which an equilibrium velocity profile becomes established, after which the mean film thickness remains constant for the remainder of the flow as does the Reynolds number defined in terms of the film thickness and the mean velocity. The investigation reported here, which was begun in association with work on heat transfer by condensation on a conical surface, sought to determine what effect a variation of Reynolds number in the flow direction might

have on the film and on the development of waves upon it.

In an early paper on condensation heat transfer, Nusselt (1) first derived the semi-parabolic velocity distribution for laminar flow in a falling film. Later Kapitza (2) obtained an approximate periodic solution of the equation of motion, and reported measurements of waves on a film on the outside of a vertical cylinder (3). Benjamin (4) in 1957 and Yih (5) in 1963 used the Navier-Stokes equations to derive equations of motion for flow over an inclined plane, and subjected these equations to a stability analysis, determining the conditions under which a disturbance of the mean flow would grow unstably. They found that such instability was a function of both Reynolds number and wave number α , and that for long waves (small α) the flow was unstable for $(Re) > 5 \tan \beta/6$. They also indicated the stabilizing influence that the presence of surface tension would have in resisting the development of unstable disturbances. The stability analysis was extended by Berbente and Ruckenstein (6) for vertical planes, and by Krantz and Goren (7) for inclined planes. In both these papers, the authors derive single parameters which are combinations of the Reynolds and Weber numbers and the slope, as indicators of the dominant wave formation to be found in the film.

The experiments reported here were carried out with a water film flowing under gravity over the surface of a vertical-axis 60° cone. As the constant volume flow spreads over the growing circumference of the cone, the mean film thickness of the film decreases. The extent of this thinning, and the consequent effect on the waves observed on the film were measured and correlated with a parameter derived from that of Berbente and Ruckenstein and clearly related to that of Krantz and Goren.

CHARACTERISTICS OF THE MEAN FILM FLOW

When the flow is laminar and sufficiently thin (i.e. at large cone radius), the film can be considered as quasi-parallel. A balance then exists between the local shear and gravitational forces:

$$\nu \frac{d^2 u}{dy^2} = -g \cos \beta$$

† Lecturer in Engineering Science, University of Durham.
The manuscript of this paper was received on 25 September 1978 and accepted for publication on 4 December 1978.

This is integrated subject to the boundary conditions of no slip at the cone surface and no shear stress at the free surface to give:

$$u = \frac{g \cos \beta}{\nu} (\delta y - \frac{1}{2}y^2) \quad (1)$$

This shows the velocity distribution to be parabolic as expected. The volumetric flow rate Q is found by integrating across the film and multiplying by the circumference of the cone at this section $2\pi x \sin \beta$:

$$Q = \frac{\pi g \sin 2\beta}{3\nu} \delta^3 x$$

From which is found the film thickness

$$\delta = \left[\frac{3\nu Q}{\pi g \sin 2\beta} \right]^{1/3} x^{-1/3} \quad (2)$$

and the mean film velocity

$$\bar{u} = \left[\frac{Q^2 g \cos \beta}{12\pi^2 \nu \sin^2 \beta} \right]^{1/3} x^{-2/3} \quad (3)$$

and hence

$$(Re) = \frac{\bar{u}\delta}{\nu} = \frac{Q}{2\pi\nu \sin \beta} x^{-1} \quad (4)$$

From these it is seen that at high values of x , δ and \bar{u} vary relatively slowly with x , thus justifying the initial quasi-parallel assumption. Distance along the cone x may be eliminated between the expression for δ and (Re) to give

$$\delta^3 = \frac{3\nu^2}{g \cos \beta} \cdot (Re) \quad (5)$$

EXPERIMENTAL METHOD

Experiments were carried out on an aluminium cone of 60° included angle and base diameter 0.6 m. The cone was fixed with its axis vertical and apex uppermost. The filtered water supply was fed upwards through a central hollow shaft. Near the apex the water flowed over a radiused weir on to the outer surface of the cone. The weir extended round the full 360° perimeter of the cone at this level, and an upper cap radiused to match the radius of the weir assisted this change of flow direction. The cone is shown in section in Fig. 1.

A capacitance method was used for the dynamic measurement of film thickness. The plane metal surface of the measurement probe was arranged parallel to and approximately 3 mm from the surface of the cone. The probe was maintained at a potential relative to the cone surface, and the instantaneous capacitance between the two measured by comparison with a standard capacitor. With a water film on the cone's surface, the capacitance measured is that of the air gap above to within 0.2 per cent, due to the high ratio of relative permittivities of water and air. So by comparison with a reading taken with no water film, the film thickness can be obtained. The capacitance comparison and output signal generation was performed by a Wayne Kerr vibration meter type DM 100. The frequency response of this system was amply good enough for the recording of these relatively

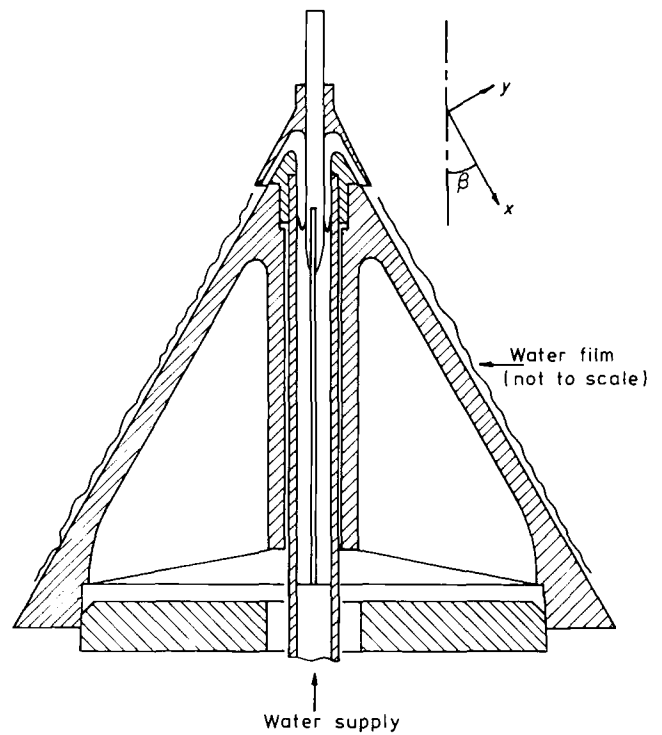


Fig. 1. Section of the experimental apparatus

low frequency variations in film thickness. The probe itself was specially designed to give good resolution of small wavelengths and yet have sufficient surface area to allow an adequate air gap and minimize the risk of wetting the probe surface. For this reason the active probe area was a long thin 'rectangle' 4.8 mm wide with semi-circular ends centred 20.8 mm apart. The shorter dimension of this probe lay parallel to the generator of the cone with the longer dimension across the flow. A large guard ring around this active surface served to maintain, as far as possible, parallel lines of flux between the probe and the cone. The error introduced by the opposition of the curved conical surface to the plane surface of the probe was calculated and found to be less than 2 per cent for the whole range of readings taken, nevertheless a computed correction was applied to all film thickness readings that would have been in error by more than 1 per cent on this count.

The output signal from the meter consisted of a d.c. component corresponding to the mean air gap, plus a small fluctuation corresponding to the variation of that gap caused by surface waves. The d.c. component was measured using a voltmeter with internal damping circuits to give a measure of mean film thickness. This output had been calibrated previously against the air gap above a static water film in a flat aluminium dish. A differential amplifier was then used to subtract the greater part of the d.c. component and provide a suitably amplified signal for feeding to an ultra-violet recorder. Typical sample waveform traces are shown in Fig. 2.

Measurements of wavelength and wave speed were obtained from a frame-by-frame analysis of a cine film record of the flow. The film was taken with a variable framing rate camera operating at typically 30–50 frames/second. Measurements were made by reference to a scale immediately above the water film that was included in the field of view of the camera, thus obviat-

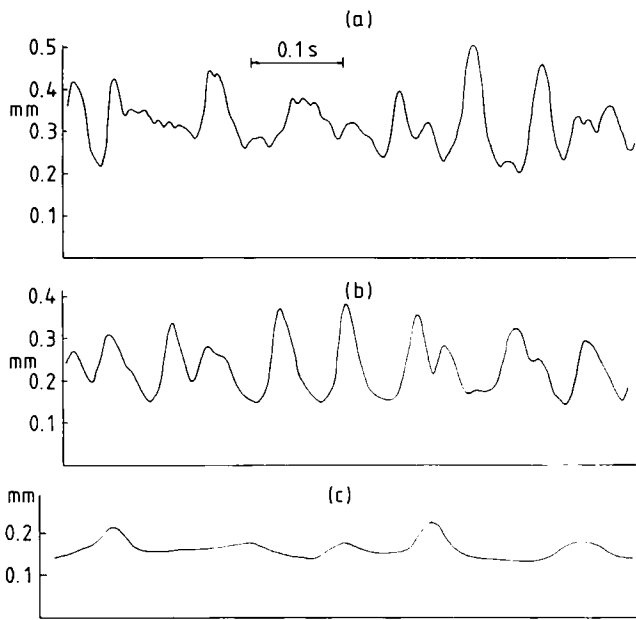


Fig. 2. Sample waveform traces

- (a) Flowrate $126 \times 10^{-6} \text{ m}^3/\text{s}$; $D = 400 \text{ mm}$; $(Re) = 91.6$
- (b) Flowrate $50.4 \times 10^{-6} \text{ m}^3/\text{s}$; $D = 400 \text{ mm}$; $(Re) = 36.6$
- (c) Flowrate $12.6 \times 10^{-6} \text{ m}^3/\text{s}$; $D = 440 \text{ mm}$; $(Re) = 7.8$

ing the need for carefully controlled enlargement factors. Careful positioning of the lighting and high contrast development were necessary to ensure good clear photographs of the smaller waves at low flowrates.

MEAN FILM THICKNESS

Figure 3 shows the mean film thickness δ plotted against (Re) for flows in the range $Q = 12.6 \times 10^{-6}$ to $126 \times 10^{-6} \text{ m}^3/\text{s}$. The full line indicates the mean film thickness predicted by eq. (5) above, i.e. $\delta_{mm} = 0.071 (Re)^{1/3}$. The dashed line is the line of best

fit, $\delta_{mm} = 0.0685 (Re)^{1/3}$. This shows good agreement on the $\frac{1}{3}$ gradient, but film thickness is $3\frac{1}{2}$ per cent less than predicted. To this must be added a further 4 per cent, the amount by which flow along the generator of the cone where measurements were taken exceeded the mean flow around the cone. Despite careful levelling of the cone, such a variation in circumferential distribution of the flow had proved unavoidable. Other tests with photographic observation of dye streams showed no detectable lateral flow. The distribution of flow was found to vary with total flowrate, the variation at the highest flowrate used being less than 0.5 per cent, while at the lowest flowrate, flow along the measurement generator exceeded the mean by almost 7 per cent. For the major part of the total flow range however the above quoted 4 per cent excess was accurate to $\pm \frac{1}{2}$ per cent.

Thus the measured mean film thickness was found to be on average $7\frac{1}{2}$ per cent less than the predicted thickness of an undisturbed laminar film. This is in good agreement with the figure of 7 per cent deduced by Kapitza (2) for the difference between an undisturbed laminar film on a vertical plane, and such a film with a superimposed steady sinusoidal undulation. This suggests that Kapitza's figure, arrived at by considering a simple sinusoidal variation of the free surface, provides a good basis for the estimation of mean film thickness in cases where the film is not only modified by a less regular wave pattern but also slowly thinning.

WAVE AMPLITUDE

As can be seen from Fig. 2, the traces of instantaneous film thickness obtained were complex. At higher Reynolds numbers, 50-200, they were jagged and showed little obvious periodicity. At intermediate values, 10-50, the variation was smoother, and a harmonic variation more clearly apparent. This was not truly regular, however, the period between wave crests varying quite

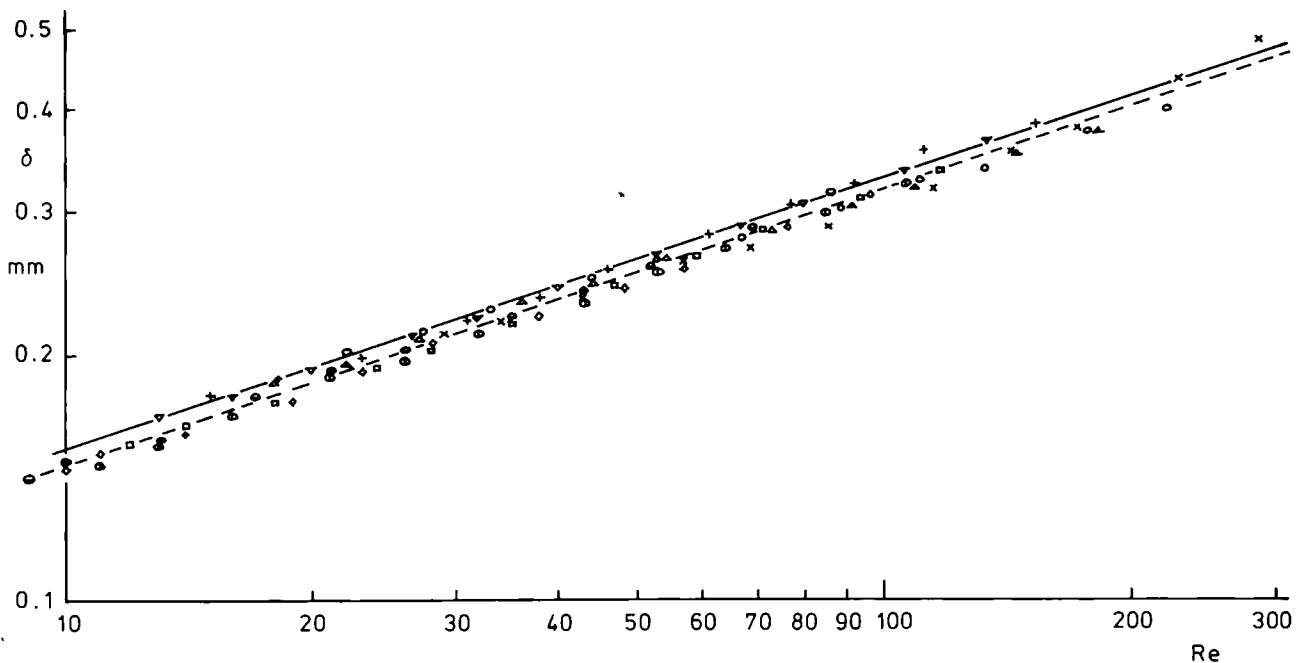


Fig. 3. Mean film thickness δ versus Reynolds number

- indicates the undisturbed laminar film thickness given by $\delta^3 = (3\nu^2/g \cos \beta) (Re)$, i.e. $\delta = 0.071 (Re)^{1/3}$ for the tests carried out
- - - indicates the line of best fit $\delta = 0.0685 (Re)^{1/3}$
- Diameters \times 140 mm, \circ 180 mm, Δ 220 mm, $+$ 260 mm, ∇ 300 mm, \square 340 mm, \oplus 380 mm, \diamond 420 mm, \bullet 460 mm

markedly. At low Reynolds number, < 10 , the waveform was found to reduce to single waves at irregular intervals. Because of the irregularity of the waveforms, three separate amplitude measures have been used. Peak amplitude \hat{A} was obtained by subtracting the mean thickness in the two lowest troughs observed in a trace of between 20 to 30 waves from the mean of the two highest peaks, and dividing the result by 2. It was observed by following the separate behaviour of peaks and troughs down the cone that peak thickness remained almost constant and that thinning of the film occurred principally in the troughs. A Fourier analysis of similar lengths of trace was carried out from which the root mean square amplitude A_{rms} was obtained. Finally a nondimensional amplitude factor, wave intensity I , was obtained by dividing A_{rms} by the mean film thickness given as the leading term of the Fourier analysis.

The variation of these three measures of amplitude with passage down the cone is shown in Figs. 4, 5 and 6 in which amplitude is plotted against the cone diameter D which for a 60° cone is equal to the distance along the generator from the apex. Figure 4 shows that the peak amplitude \hat{A} is clearly dependent on flowrate, and reaches a maximum value at a distance down the cone which increases with increasing flowrate. The root mean square amplitude obtained by Fourier analysis and shown in Fig. 5 behaves somewhat similarly. That the peak and subsequent decline are more pronounced at low flowrates, suggests a concentration of energy into a dominant wave frequency that tends to maintain the peak amplitude while the r.m.s. value decreases more rapidly with the decay of the other wave frequencies. This is supported by observations of recorder traces which appear to become more regular as the waves progress down the cone, and cine film which shows small-

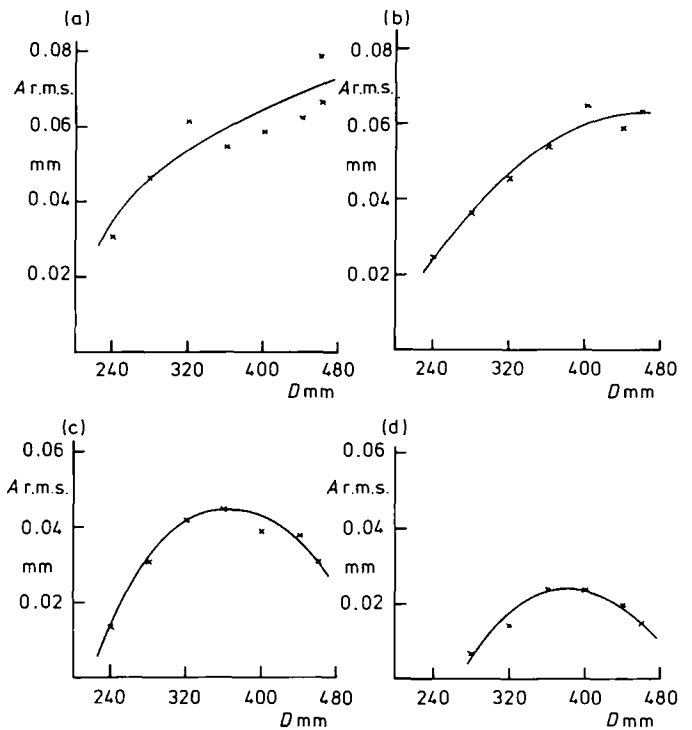


Fig. 5. Root mean square wave amplitude A_{rms} versus diameter D
 Flowrates: (a) $126 \times 10^{-6} \text{ m}^3/\text{s}$; (b) $50.4 \times 10^{-6} \text{ m}^3/\text{s}$;
 (c) $25.2 \times 10^{-6} \text{ m}^3/\text{s}$; (d) $12.6 \times 10^{-6} \text{ m}^3/\text{s}$.

er wavefronts being overtaken and engulfed by the larger ones. Figure 6 shows the variation of the wave intensity I . Kapitza predicted theoretically that intensity I would have a limiting constant value of 0.23 for a sinusoidal wave on a film of constant mean thickness. Figure 6 shows that neither this single value nor the value of

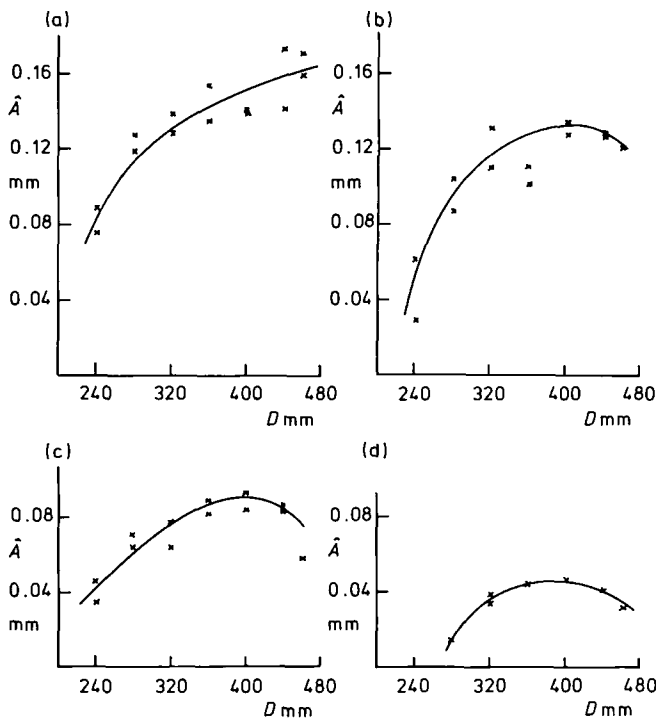


Fig. 4. Peak amplitude \hat{A} versus diameter D
 Flowrates: (a) $126 \times 10^{-6} \text{ m}^3/\text{s}$; (b) $50.4 \times 10^{-6} \text{ m}^3/\text{s}$;
 (c) $25.2 \times 10^{-6} \text{ m}^3/\text{s}$; (d) $12.6 \times 10^{-6} \text{ m}^3/\text{s}$.

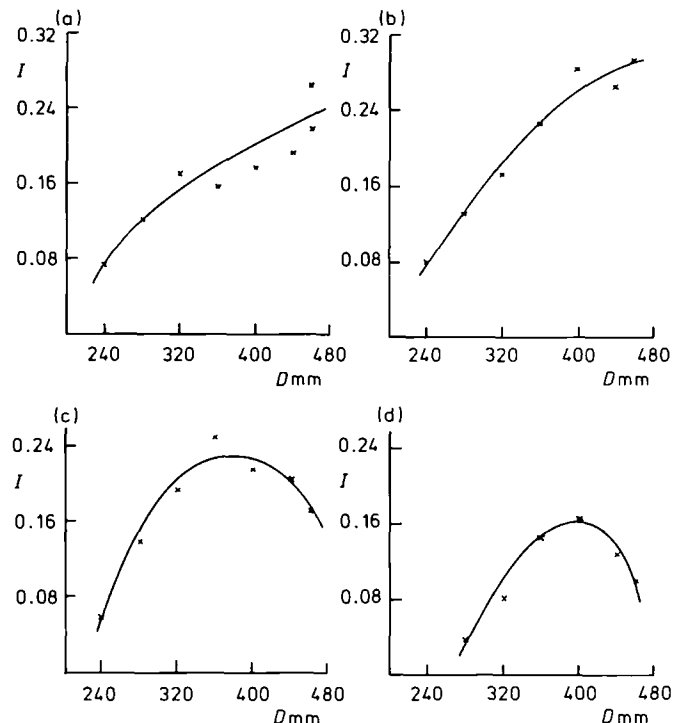


Fig. 6. Wave intensity I versus diameter D
 Flowrates: (a) $126 \times 10^{-6} \text{ m}^3/\text{s}$; (b) $50.4 \times 10^{-6} \text{ m}^3/\text{s}$;
 (c) $25.2 \times 10^{-6} \text{ m}^3/\text{s}$; (d) $12.6 \times 10^{-6} \text{ m}^3/\text{s}$.

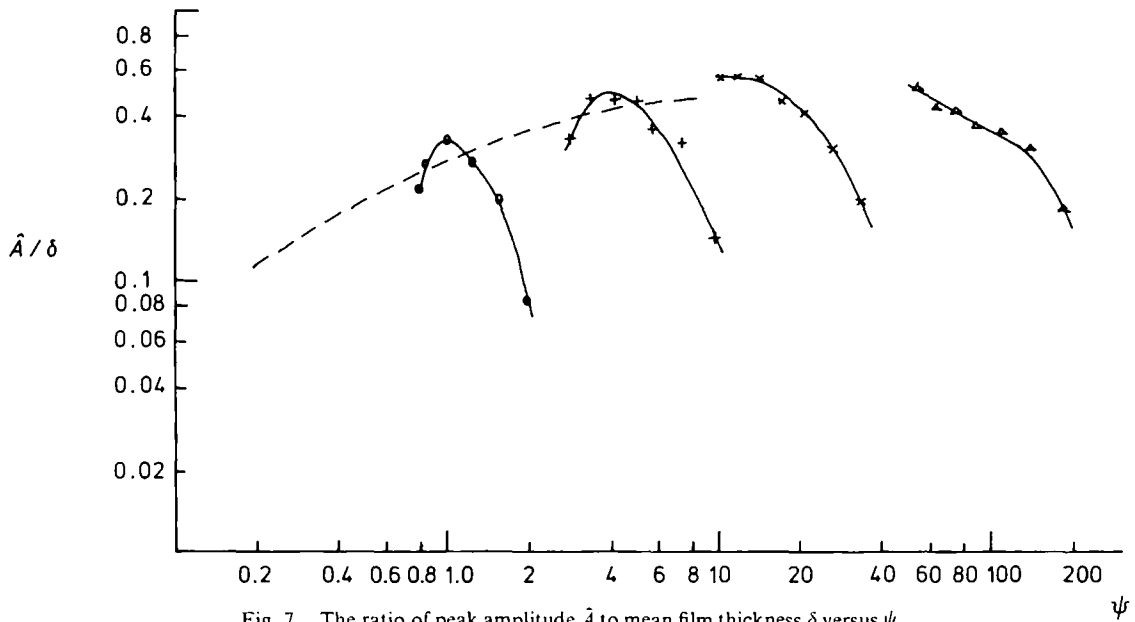


Fig. 7. The ratio of peak amplitude \hat{A} to mean film thickness δ versus ψ
 ----- indicates the variation as predicted by Berbente and Ruckenstein
 Flowrates: (a) $126 \times 10^{-6} \text{ m}^3/\text{s}$ Δ ; (b) $50.4 \times 10^{-6} \text{ m}^3/\text{s}$ \times ; (c) $25.2 \times 10^{-6} \text{ m}^3/\text{s}$ $+$; (d) $12.6 \times 10^{-6} \text{ m}^3/\text{s}$ \circ .

0.29 later proposed by Bushmanov (8) adequately describes the flow studied.

All three amplitude plots do however point to the conclusion that as flow progresses down the surface of the cone, amplitude increases with the amplification of disturbances until a limiting amplitude is reached, after which this limiting amplitude decreases as the film thins; and that the greater the flowrate the greater the distance required for the growing wave to reach its peak amplitude.

Berbente and Ruckenstein (6) suggest a form for the dependence of this limiting amplitude in terms of a non-dimensional group ψ which may be reduced from the complex form in which they present it, to

$$\psi = (Re)^{7/6} (Fr)^{-1/3} (We)$$

It is thus seen to be a combination of the Reynolds, Weber, and Froude numbers for the flow. For the flow studied here it can be shown from eqs. (2), (3) and (4), above that the Reynolds and Froude numbers are linked by the relationship

$$3 (Fr)^2 = (Re) \cos \beta$$

so that

$$\psi = \left(\frac{3}{\cos \beta} \right)^{1/6} (Re) (We)$$

This is similar to a group suggested by Krantz and Goren (7)

$$\psi' = \frac{(\frac{6}{5} (Re) - \tan \beta)^3}{(Re)} (We)^2$$

The latter makes a more direct allowance for the effect of slope which they had included in their considerations (Berbente and Ruckenstein had considered a vertical plane only; the slope term arises from the author's relationship between (Fr) and (Re) which takes into account the reduced gravitational component along the plane).

However the effect of β is small unless either β approaches $\pi/2$ or (Re) is very small. If neither is the case then ψ' reduces to a group closely similar to that derived from the one of Berbente and Ruckenstein, and for the cone studied ($\beta = 30^\circ$)

$$\psi' = 1.142\psi^2$$

Figure 7 shows the nondimensional peak amplitude \hat{A}/δ plotted against ψ for the flowrates studied together with the relationship derived by Berbente and Ruckenstein, which was based on the results of Kapitza and Kapitza (3). Better agreement is found than with the relationship derived by Anshus (9) reported by Krantz and Goren (7). The latter relationship predicts a limiting nondimensional amplitude of approximately 1.0 for the whole of the range of ψ shown. Results of experiments with oils of low surface tension by Krantz and Goren gave good agreement with the theory of Anshus; but the results of Kapitza and Kapitza, and now those presented here, do not. Krantz and Goren sought to explain this lack of agreement in terms of fluid impurities that might have affected the surface tension. However, the results of the Kapitzas—who used distilled water—and those of the author—obtained with ordinary tap water—are closely similar. This would seem to suggest that some other explanation is required to satisfy this discrepancy.

While the results obtained on the cone fit the Berbente and Ruckenstein planar prediction well so far as the maximum value of amplitude is concerned, the behaviour at points further down the surface is less readily explained. It might be expected that once the waves had reached their limiting amplitude this amplitude would then continue to be controlled by the Reynolds number of the flow. This would appear on the graph as a rise to the limiting curve with decreasing Reynolds number followed by a fall along the limiting curve after it had been reached, with a possible lag in the decreasing amplitude. The results obtained show a decline of amplitude more rapid than that expected. This final point

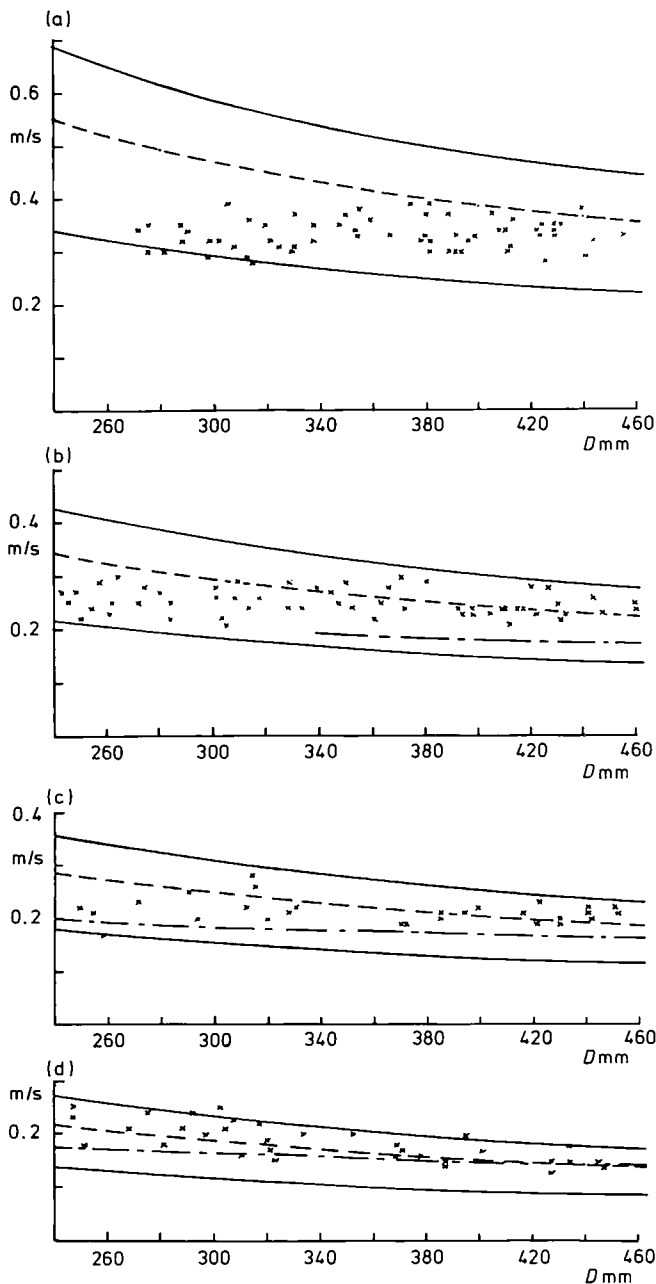


Fig. 8. Wave speed versus diameter D

The upper and lower full lines indicate respectively 3 times and 1.5 times the mean film speed

----- indicates 2.4 times the mean film speed, the wave speed as predicted by Kapitza

- · - · indicates the wave speed predicted by Berbente and Ruckenstein

Flowrates: (a) $50.4 \times 10^{-6} \text{ m}^3/\text{s}$; (b) $25.2 \times 10^{-6} \text{ m}^3/\text{s}$;

(c) $18.9 \times 10^{-6} \text{ m}^3/\text{s}$; (d) $12.6 \times 10^{-6} \text{ m}^3/\text{s}$.

must not however be treated with undue emphasis, since the number of points on the graph suggesting it are small and they are the ones for which the film was thinnest and experimental error consequently highest.

WAVE SPEED

Benjamin (4) quoting the work of Lighthill and Whitham (10) showed the velocity of a long kinematic wave to be three times the mean velocity in the film on an inclined plane. Although the waves observed had wavelengths of up to 100δ some departure from the

factor three might be expected especially for still-developing waves on a cone. Kapitza (2) derived a wave speed of 2.4 times mean film speed for sinusoidal waves on a film of constant mean thickness. Figure 8 shows measured wave speeds against D , cone diameter, for four different flowrates. While there is considerable scatter, the results suggest quite clearly that a developing wave progresses down the cone with a fixed velocity until that velocity approaches the value of 3 \times mean film velocity, whereafter the wave velocity decreases in line with the decreasing mean film velocity. The readings show the factor of 3 as being somewhat high, and equally Kapitza's 2.4 as being low for the ratio of wave speed to mean film speed.

Also shown, where calculable from the values presented, is a prediction of wave velocity given by Berbente and Ruckenstein (6) which was based partly on analysis and partly on the Kapitza's results. This is seen to agree far less well with the author's observations than did their limiting amplitude predictions.

WAVELENGTH AND WAVE NUMBER

Figure 9 shows the variation of wavelength with cone diameter D for different flowrates. The pattern that emerges is one of wavelength increasing with passage down the cone, and doing so more rapidly with lower flowrates and with waveforms that have reached their

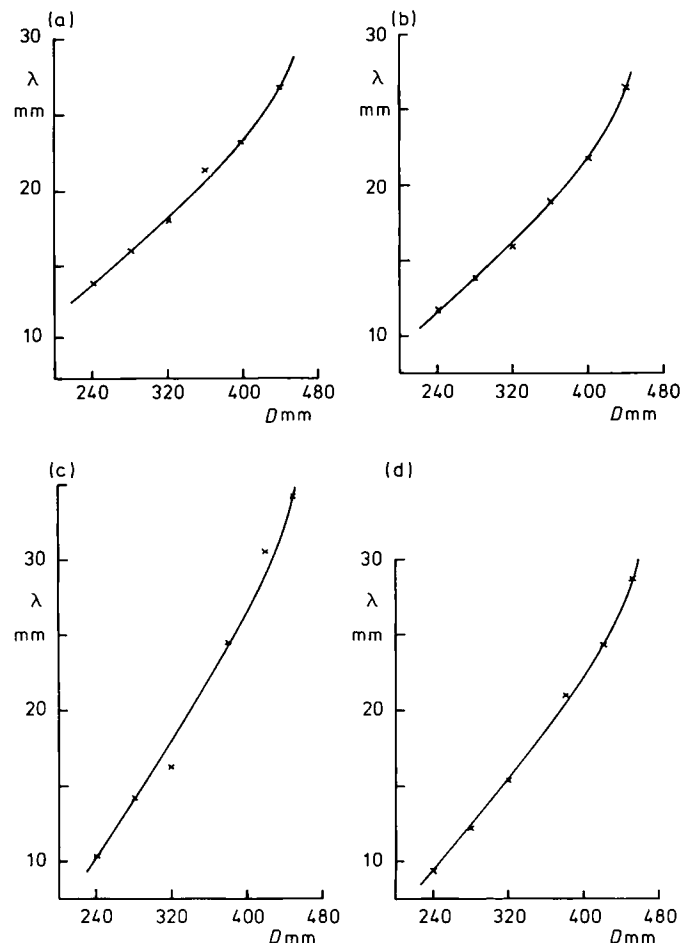


Fig. 9. Variation of wavelength λ with diameter D

Flowrates: (a) $50.4 \times 10^{-6} \text{ m}^3/\text{s}$; (b) $25.2 \times 10^{-6} \text{ m}^3/\text{s}$;

(c) $18.9 \times 10^{-6} \text{ m}^3/\text{s}$; (d) $12.6 \times 10^{-6} \text{ m}^3/\text{s}$.

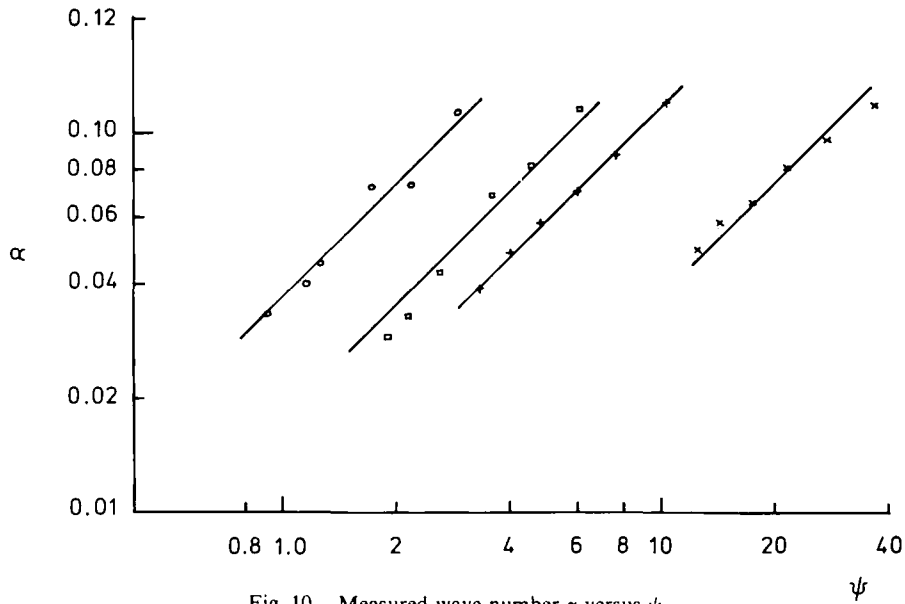


Fig. 10. Measured wave number α versus ψ
 Flowrates: $\times Q = 50.4 \times 10^{-6} \text{ m}^3/\text{s}$; $+ Q = 25.2 \times 10^{-6} \text{ m}^3/\text{s}$; $\square Q = 18.9 \times 10^{-6} \text{ m}^3/\text{s}$; $\circ Q = 12.6 \times 10^{-6} \text{ m}^3/\text{s}$.

limiting amplitude. Up to this point the rate of increase is almost linear.

The nonuniformity of the wavefronts apparent in the traces shown in Fig. 2, and in visual observation that showed fronts to be curved and overlapping rather than regularly parallel to one another, made wavelength measurements difficult. The measurements plotted in Fig. 9 are the means of several individual measurements of distances between parallel portions of wavefront obtained from photographs. A secondary check on these values was obtained by calculating the wavelength from values obtained for wavespeed and the dominant frequency of wave passage obtained from a computed spectral density obtained along with the Fourier analysis of the ultra-violet recorder traces. The spectral densities thus obtained, while not showing a single clearly defined peak value of energy at a single frequency, did show a concentration of energy around a mean frequency that clearly decreased with passage down the cone, and was smaller at lower flowrates. Frequencies of 12–21 Hz dropping to 6–12 Hz between diameters 280 and 460 mm were thus obtained. These check values of wavelength gave effective corroboration of the trends reported above although the values obtained were up to 15 per cent higher.

The non-dimensional measure of wavelength, the wave number $\alpha (= 2\pi\delta/\lambda)$ calculated from the mean of the two values of λ obtained and a corresponding value of mean thickness for the film, calculated from $\delta = 0.0685 (Re)^{1/3}$, is shown in Fig. 10 plotted against the parameter ψ for four different values of flowrate Q . These points, plotted logarithmically to accommodate the range of ψ , indicate strongly a direct relationship between α and ψ for a given flowrate. Further investigation of the part played by flowrate in the relationship leads to an empirical predictive relationship between α , ψ and Q in the form

$$\alpha = 1.5 \times 10^{-9} \psi / Q^{3/2}$$

where Q is in m^3/s . Figure 11 shows the measured values of α for all four flowrates plotted against the value arising

from the above relationship. Perfect agreement would cause all points to fall on the 45° line drawn. While this is clearly not achieved, the clear majority of points are seen to lie within the ± 10 per cent lines. Of the points falling outside this band, the three points at higher α correspond to flows high up on the cone where the developing waves were only barely visible, and the two lowest points were at the $18.9 \times 10^{-6} \text{ m}^3/\text{s}$ flowrate for which the film thickness was small and only a single estimate of α was available since spectrum analysis of waves at this flowrate had not been carried out.

The range of wave number encountered at each flowrate is seen to be quite similar. Only at wave num-

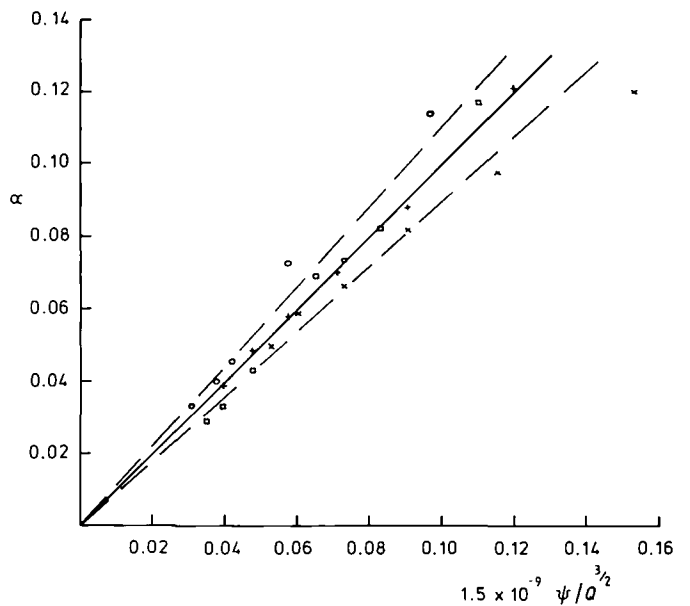


Fig. 11. Measured wave number α versus the wave number predicted by the relationship $\alpha = 1.5 \times 10^{-9} \psi / Q^{3/2}$
 — indicates the line of equality between measured and predicted values
 - - - indicates the lines of $\pm 10\%$
 Flowrates: $\times Q = 50.4 \times 10^{-6} \text{ m}^3/\text{s}$; $+ Q = 25.2 \times 10^{-6} \text{ m}^3/\text{s}$; $\square Q = 18.9 \times 10^{-6} \text{ m}^3/\text{s}$; $\circ Q = 12.6 \times 10^{-6} \text{ m}^3/\text{s}$.

Table 1

Criterion	α		
	$Q = 50.4$	$Q = 25.2$	$Q = 12.6 \times 10^{-6} \text{ m}^3/\text{s}$
max \hat{A}	0.058	0.048	0.047
max A_{rms}	0.047	0.057	0.049
max I		0.054	0.042
max \hat{A}/δ	0.043	0.049	0.037

bers of 0.12 or less were waves sensibly detectable on the surface. There is some evidence to support the idea that the growth of the waves ceases at a single value of wave number too. Taking maximum values of \hat{A} , A_{rms} and I , plus the maxima shown in Fig. 7 as criteria to determine when the limiting amplitude is reached, the corresponding values of α for the flowrates 50.4, 25.2 and $12.6 \times 10^{-6} \text{ m}^3/\text{s}$ are given in Table 1.

If the three extreme values of α listed in Table 1 are discounted, the remaining eight values have a mean of 0.048 and all fall within $\pm 12\frac{1}{2}$ per cent of that value. Therefore for flow of water on the 60° cone three regions of flow were found in terms of α :

$\alpha > 0.120$ no measurable waves found
 $0.120 > \alpha > 0.048$ waves amplifying
 $0.048 > \alpha$ waves past their limiting amplitude and decaying with thinning of the mean film.

CONCLUSIONS

1. Waves are found to form on the film of water flowing under gravity over the surface of the 60° cone. They grow to a limiting amplitude and then decay with further progress and thinning of the film. The distance required for a limiting amplitude to be reached increases with flowrate.

2. The mean film thickness was found to be $7\frac{1}{2}$ per cent less than that predicted for a laminar film without waves, eqs. 2 and 5. This is in good agreement with a value deduced by Kapitza (2) for flow down a plane vertical surface.

3. The limiting amplitude reached by the waves agrees well with that predicted by the theory of Berbente and Ruckenstein (6) which was again developed for a plane vertical surface. After the limiting amplitude is reached, the wave amplitude decreases. The non-dimensional parameters ψ and ψ' proposed by Berbente and Ruckenstein, and by Krantz and Goren (7) are shown to be similar for non-extreme values of slope. The correlation obtained shows that limiting amplitude depends on the local value of both the Reynolds number and the Weber number.

4. Wave speed remains constant until it approaches a value of three times the mean velocity of the decelerating thinning film. The wave speed then falls, remaining at between 2.4 and 3 times the mean film velocity.

5. Wavelength increases with passage down the cone.

6. The wave number is given empirically by $\alpha = 1.5 \times 10^{-9} \psi/Q^{3/2}$. For low flowrates the value of α at which waves are first detectable is 0.12 after which α decreases as the wave amplitude grows until limiting amplitude is reached at a value of α in the region of 0.048. At lower values of α the waves are decaying in amplitude.

REFERENCES

- (1) NUSSELT, W. 'Oberflächen Condensation des Wasserdampfs', *Z. Ver. dt. Ing.* 1916, **60**, 541 and 569.
- (2) KAPITZA, P. L. 'Wave Motion of a Thin Layer of a Viscous Liquid—Part I', *Zh. eksp. teor. Fiz.* 1948, **18**, 3
- (3) KAPITZA, P. L. and KAPITZA, S. P. 'Wave Motion of a Thin Layer of a Viscous Liquid—Part III', *Zh. eksp. teor. Fiz.* 1949, **19**, 105
- (4) BENJAMIN, T. BROOKE. 'Wave Formation in Laminar Flow down an Inclined Plane', *J. Fluid Mech.* 1957, **2**, 554
- (5) YIH, C-S. 'Stability of Liquid Flow down an Inclined Plane', *Physics Fluids.* 1963, **6**, 321
- (6) BERBENTE, C. P. and RUCKENSTEIN, E. 'Hydrodynamics of Wave Flow', *A.I.Ch.E.J.* 1968, **14**, 772
- (7) KRANTZ, W. B. and GOREN, S. L. 'Finite Amplitude Long Waves on Liquid Films Flowing down an Inclined Plane', *Ind. Engng. Chem. Fundamentals.* 1970, **9**, 107
- (8) BUSHMANOV, C. K. 'Hydrodynamic Stability of a Liquid Layer on a Vertical Wall', *Soviet Phys. JETP.* 1961, **12**, 873
- (9) ANSHUS, B. E. Ph.D. Thesis, Univ. of California, Berkeley, 1965
- (10) LIGHTHILL, M. J. and WHITHAM, G. B. 'On Kinematic Waves', *Proc. R. Soc.* 1955, **A229**, 281